Volume 1 | Number 1 | Jan 2013 | Pages 1–100

Journal of
Materials Chemistry C

Materials for optical and electronic devices
www.rsc.org/materialsC

ROYAL SOCIETY
OF CHEMISTRY

ROYAL SOCIETY
OF CHEMISTRY

www.rsc.org/materialsC

ARTICLE TYPE

Electrochemical Co-deposition of Sol-Gel/Carbon Nanotubes Composite Thin Films for Antireflection and Non-Linear Optics

Liang Liu[a, b], Shai Yellinek[a], Noam Tal[a], Reut Toledano[a], Ariela Donval[c], Doron Yadlovker[d] and Daniel Mandler*[a]

Sol-gel/carbon nanotubes (CNTs) nano-composite films were electrochemically deposited by applying negative potential to a conducting substrate, *i.e.* indium tin oxide (ITO) and Ag grid printed on polyethylene terephthalate (PET). The deposition is driven by the local pH rise on the cathode that 10 catalyzes the formation of sol-gel films. The latter serves as binder and entrapment for CNTs. The deposition can be well manipulated by deposition potential and time, and the film can be selectively electrodeposited on the conductive parts of Ag grids printed on PET from an optimized dispersion. The thickness, transmittance, morphology and hydrophilicity of the films are characterized by profilometry, spectrophotometer, scanning electron microscopy (SEM) and water contact angle, respectively. It is 15 further revealed that the electrodeposited sol-gel/CNTs composite films have non-linear optical properties and exhibit pronounced antireflective performance (specular reflection < 0.5% over visible to long-wave IR range, allowing their potential applications as optical materials.

Introduction

The unique chemical and physical properties of carbon nanotubes 20 (CNTs) have channeled substantial efforts to embedding them into different matrices. The resulting materials, which can be in the form of nano-composites or nano-hybrids exhibit improved characteristics such as conductivity, electrical capacity, mechanical strength and non-linear optics[1-3]. Many of the studies 25 comprising the incorporation of CNTs into various matrices aim at formation of thin films, where the foreseen applications are in a wide variety of areas including solar cells[4], electromechanical actuators[5], supercapacitors[6], gas sensors[7], photocatalysis[8-10] and field emission devices[11].

30 It is interesting to review the different types of materials used to accommodate CNTs. The latter span from organic to inorganic polymers[12, 13] and include also conducting polymers[14], metal oxides[15], sol-gel materials[16], and even metals[17]. A wide variety of organic polymers have been exploited in conjunction with 35 CNTs[12, 18-21]. For example, nano-composites made of polymethylmethacrylate/CNTs exhibit organic semiconductor behavior[22] whereas polyimide/CNTs composite films showed improved electrical conductivity and thermal properties[13]. Numerous studies focused on the formation of conducting 40 polymers/CNTs composites where the electrochemical preparation method, *i.e.* electropolymerization appeared to be highly promising for obtaining superior properties[23-25]. Baibarac *et al.* reviewed[14] this area of nano-composite materials formed by conducting organic polymers and CNTs. They presented two 45 types of nano-composites: conductive polymers functionalized CNTs and conductive polymers doped with CNTs.

As mentioned above, efforts have also been made towards the preparation of a variety of hybrid and composite materials based on CNTs and inorganic oxides, such as SiO_2, TiO_2, SnO_2 and 50 $ZnO^{15, 26-29}$. Eder[30] reviewed these studies, where CNTs were combined with a variety of inorganic compounds primarily oxides, yet also nitrides, carbides, chalcogenides and ceramics. He concluded that there are still unresolved challenges in this new developing area, such as controlling the interface, 55 morphology and phase composition as well as the effect of the type and quality of the CNTs on the resulting composite materials.

Silica compounds are extensively studied materials, mainly those prepared by the sol-gel process[31, 32]. Sol-gel derived silica/CNT 60 composites have been primarily used for biosensing, optics and reinforcement of thin films[33-36]. For example, covalent bonding between the nanotubes and the silica matrix, resulted in improved interfacial interactions and due to that improvement, covalent filling of the SWCNTs in silica achieved both enhanced strength 65 and toughness[33].

Sol-gel/CNTs nano-composites have primarily been prepared by conventional wet methods that include dip- and spin-coating, spraying and casting. We have developed a method for the electrochemical deposition of sol-gel[37]. The technique is based on 70 the hydrolysis of a metal alkoxide carried out under low pH, which is followed by the application of negative potential to an electrode surface which caused local increase of the pH and catalyzed the condensation process. This approach has been utilized by other laboratories[38-42] as well. More recently, this 75 approach has been expanded to form silica based composite films by the co-deposition of sol-gel precursors and various materials. For example, metal ions, *e.g.* Cu^{2+} and Zn^{2+} were electrochemically co-deposited with the sol-gel to form composite films[43, 44]. Au nanoparticles were also co-deposited 80 with sol-gel resulting in the formation of Au nanoparticles embedded in a sol-gel matrix[45].

A few studies were reported regarding the electrodeposition of sol-gel and CNTs[46, 47]. Wong and his coworkers[46] developed two approaches for the deposition of silica onto SWCNT. The first procedure involved the direct deposition of silica as a result of applying negative potentials onto a SWCNT surface. The other approach was based on increasing the pH in the solution, which consisted of SWCNT and a silane precursor, using a Pt electrode. The silica that was formed wrapped the nanotubes and precipitated in the solution from which they were filtered and collected. Walcarius *et al*[47]. co-electrodeposited sol-gel, carboxylic functionalized SWCNTs modified with vitamin K3, and enzymes for electroanalysis, but the concentration of CNTs in their deposition solution was very low (0.05-0.1 wt.%). It is worth mentioning also the study by Yang *et al.*[48] who succeeded to electrochemically deposit carboxylic functionalized multi-walled carbon nanotubes (MWCNTs) in the absence of surfactants, polymers or sol-gel materials. The deposition was driven by pH decrease on the ITO anode which caused carboxylic functionalized MWCNTs to precipitate. Recently, Carzola-Amorós and co-workers[49] reported the electro-assisted deposition of carboxylic functionalized CNTs in a glass capillary tube based on the same approach. Note that these approaches are only applicable for carboxylic functionalized CNTs.

Here, we report a simple, fast and controllable approach where sol-gel/CNTs nano-composite thin films were prepared in a single electrochemical step. As compared with previous reports, an optimized dispersion consisting of sol-gel precursor and much higher concentration of unmodified MWCNTs (0.5 wt.%) was used for electrochemical deposition. The films were cathodically electrodeposited and the growth of the films was controlled by the applied potential and time of deposition. Selective deposition was achieved on conductive Ag surface that was printed on insulating polyethylene terephthalate (PET). Moreover, the electrodeposited films on ITO exhibited non-linear optical response, and the films on Ag could be used as antireflective coatings. This suggests electrodeposition as a powerful method for preparing sol-gel/CNT composite films for optical applications.

Experimental Section

Materials and chemicals: Tetramethoxysilane (TMOS, 98%, Merck), N-methylpyrrolidone (NMP, 99%, Sigma-Aldrich) and MWCNTs (Cheap Tubes) and a surfactant were used as received. Cetyltrimethylammonium nitrate (CTAN) was synthesized from cetyltrimethylammonium bromide (CTAB, 98%, Aldrich) and $AgNO_3$ (99%, Sigma-Aldrich) following protocols as shown in literature[50]. The substrates used were indium tin oxide (ITO) on glass (CG-60IN-CUV, R_S = 15-25 Ω, Delta Technologies Stillwater, MN, USA) and Ag grids/squares printed on PET (thickness of Ag: 4 μm, CPC, Israel). The ITO samples were sequentially sonicated in ethanol, 1:1 (vol. ratio) $NH_3 \cdot H_2O/H_2O_2$, and H_2O for 10, 30 and 10 min, respectively. The Ag grids/squares samples were cleaned with iso-propanol before use.

Dispersion preparation: The preparation of the deposition precursor consisted of two steps. First, MWCNTs, NMP, CTAN and H_2O were mixed to obtain a silane-free dispersion. It was then sonicated in ice/water bath with a probe sonicator (VC750, Sonics, CT, USA) at 600 W for 1 h. The MWCNTs were well dispersed after sonication, and the dispersion was stable for at least 6 months. Second, silane was added into the dispersion, which was further mixed and hydrolyzed at room temperature (~25 °C) before deposition. Two dispersions, denoted as Dispersion A and B, were used in this work. Dispersion A consisted of 0.5 wt.% MWCNT, 0.2 M TMOS, 1 wt.% CTAN and 50 vol.% NMP. It was used for electrodeposition without pre-

hydrolysis. Dispersion B consisted of the same concentration of MWCNT, TMOS and surfactant, but lower concentration of NMP. It had lower viscosity as compared with Dispersion A, but needed to hydrolyze for 12 h before electrodeposition.
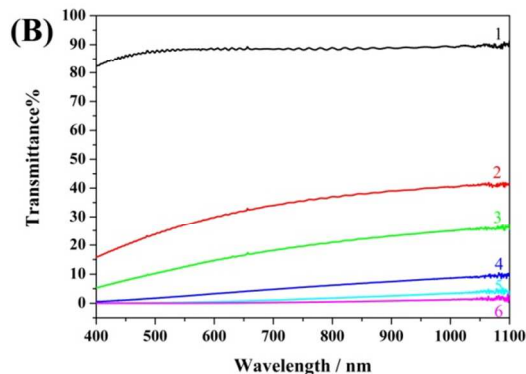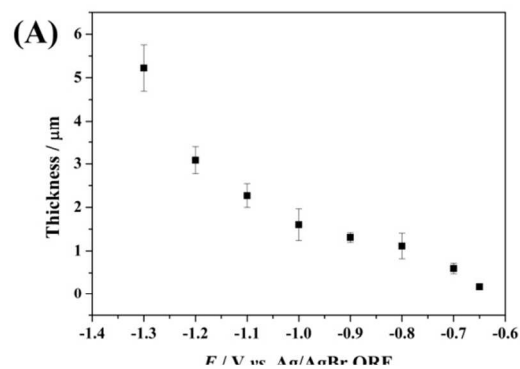
Electrodeposition: The electrodeposition was performed with a CHI 920C potentiostat (CH Instruments, USA) using a standard three-electrode cell with an Ag/AgBr wire as quasi reference electrode (Ag/AgBr QRE) and a Pt wire as counter electrode. The working electrodes were the substrates, namely ITO and Ag grids/squares on PET. A constant cathodic potential was applied to the working electrode for 0.5 to 10 min. After deposition, the films were washed thoroughly with DI water and then blow-dried with N_2 flow. The films were placed at ambient conditions overnight before characterizations.

Characterizations: Scanning electron microscopy (SEM) images were acquired with a SIRION microscope (FEI Co. Ltd.) using an electron-beam of 5 kV. Energy-dispersive X-ray mapping (EDX) was carried out with acceleration voltage of 10 kV. The thickness of the deposited films was measured with a profilometer (P-15, KLA-Tencor Co., San Jose, CA). The films were scratched with a wooden stick. The transmittance of the films in the range of 400 - 1100 nm was measured with a HP 8452A spectrophotometer. The specular reflectance of the samples was measured by a spectrophotometer (Perkin-Elmer Lambda 900 for the visible to near IR range and Perkin-Elmer 983 for the near IR to far IR range). BK7 glass was used as reference. The non-linear optical properties of the films were measured using a laser beam with wavelength of 532 nm. The diameter of the irritated area was 21 μm. Transmittance of the samples was measured as a function of the energy of the input laser.

Results and Discussion

Two approaches can be applied for successfully electrodepositing CNTs. The first involves their functionalization by carboxylic acid, as has been shown by Yang[48]. The other method comprises the entrapment of CNTs in an electrodeposited matrix such as sol-gel. We have shown that this latter approach can be applied for the electrochemical co-deposition of sol-gel with other materials such as metal ions, nanoparticles and polymers[43, 45, 51-53]. Here we examine the applicability of this method to non-functionalized CNTs.

The key essence of electrodeposition is the manipulation of the process. The properties of the electrochemically deposited films are highly dependent on the deposition conditions, such as deposition potential and time. This is of utmost importance for tuning desired optical performance. Fig. 1A shows the thickness of sol-gel/CNTs films as a function of deposition potential. Specifically, an ITO surface was immersed in a dispersion of CNTs containing TMOS and a negative potential was applied for a fixed duration of 5 min. It is evident that the thickness of the films increases upon shifting the deposition potential negative, which is in agreement with the trend seen in previous reports[37, 42]. This is due to the enhanced OH^- generation at more negative potentials. The cathodically generated OH^- ions are believed to be the main driving force for the electrodeposition of sol-gel films. Interestingly, the film thickness increases substantailly when the potential is more negative than −1.0 V. This can be explained by the exponential dependence of electrochemical reduction kinetics of water on potential.

In accordance with the increasing thickness, the transmittance of the films decreases as the deposition potential becomes negative
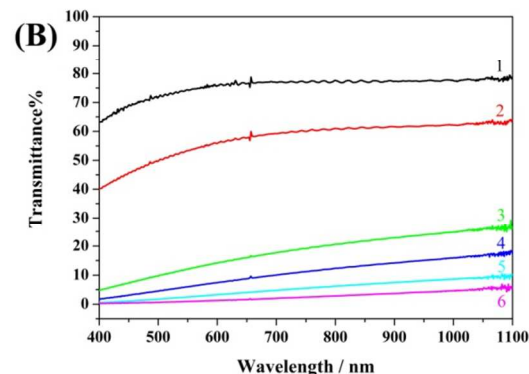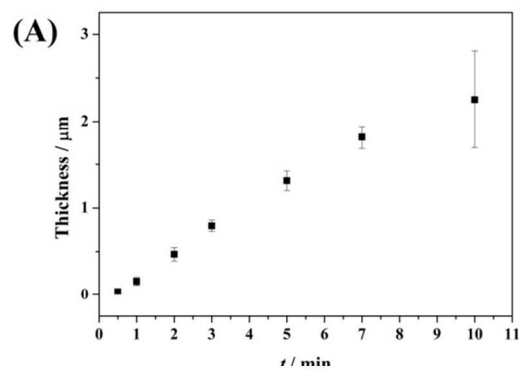
Fig. 1 Effect of deposition potential on the thickness (A) and transmittance (B) of the sol-gel/CNT composite films electrodeposited from Dispersion A. In (B) 1-6 corresponds to dip-coating and electrodeposition at −0.65, −0.7, −0.9, −1.1 and −1.3 V, respectively. Deposition time: 5 min.
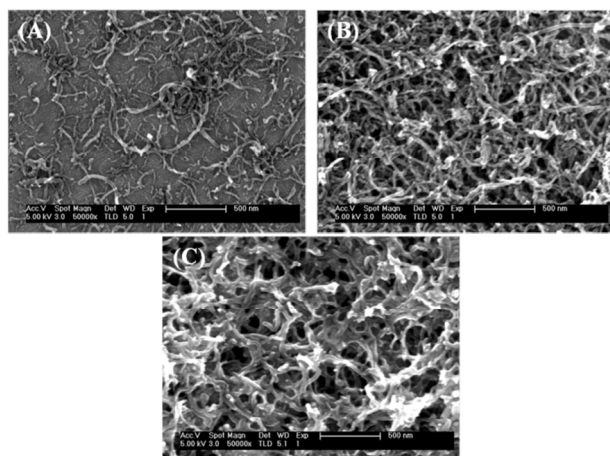
Fig. 2 SEM images of the sol-gel/CNT composite films dip-coated (A) and electrodeposited at −0.65 V (B) and −1.1 V (C) for 5 min from Dispersion A.

(Fig. 1B). The films prepared at potentials more negative than −1.1 V are almost completely non-transparent. It should be noted that the dip-coated sample appears to be light brown, having transmittance of *ca.* 88%. This indicates that only a very thin sol-gel/CNT composite film can be dip-coated on ITO surface, probably due to the high viscosity of Dispersion A.

Fig. 2 displays the SEM images of sol-gel/CNT composite films

Fig. 3 Effect of deposition time on the thickness (A) and transmittance (B) of the sol-gel/CNT composite films electrodeposited from Dispersion A. In (B) 1-6 corresponds to 0.5, 1, 2, 3, 5 and 10 min, respectively. Deposition potential: −0.9 V.

electrodeposited at different potentials. Only sparsely distributed CNTs are seen on the dip-coated sample (Fig. 2A). This confirms the dip-coating of the film, which leads to the light brown color and slight decrease in the transmittance of the sample (Fig. 1B). As compared with the dip-coated sample, the film electrodeposited at −0.65 V contains much denser CNTs, indicating that even electrodeposition at mild negative potentials could significantly facilitate the film formation (Fig. 2B). The increase in the CNT density may arise from the electrodeposited thin layer of silane film, which acts as a binder, although the silane component is not clearly observed in the image. From Fig. 2C, it is clearly seen that the CNTs are embedded within the silane. This suggests significant sol-gel film formation at very negative potentials, which is in agreement with the high thickness of the film. EDX analysis confirms the presence and increase of carbon and silicon signals with film thickness; however these data (not shown) must be taken cautiously (and are not quantitative) as carbon can be contributed by contamination and the silicon signal is also affected by the glass below ITO. Since the CNTs are conductive, the sol-gel film could also be electrodeposited on their surface, leading to the morphology shown in Fig. 2C.

The effect of deposition time on the thickness and transmittance of sol-gel/CNT composite films was also examined. Fig. 3 shows that the films grow thicker upon extending the deposition time. Correspondingly, the transmittance of the films gradually decreases. This trend is in agreement with the literature and our
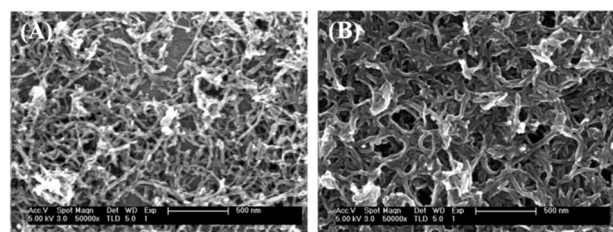
Fig. 4 SEM images of the sol-gel/CNT composite films electrodeposited at −0.9 V for 1 min (A) and 10 min (B) from Dispersion A.
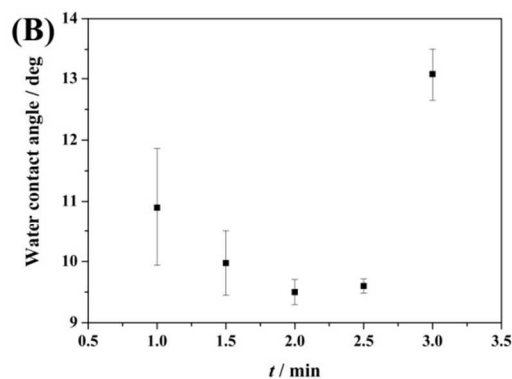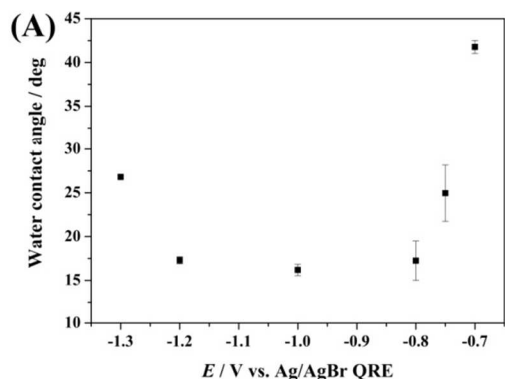

Fig. 5 Effect of deposition potential (A) and time (B) on the water contact angle of the sol-gel/CNT composite films electrodeposited from Dispersion B.

previous works regarding electrodeposition of sol-gel films,
[10] which is due to the enhanced cathodic accumulation of OH⁻ ions with long deposition time. The enhancement in sol-gel deposition is confirmed by SEM images (Fig. 4). It is seen that the film electrodeposited for 1 min consists of mainly CNTs, while the film electrodeposited for 10 min shows CNTs embedded within
[15] the sol-gel film similarly to Fig. 2C.

The results above suggest that sol-gel/CNT composite films can be electrodeposited upon applying negative potential to the ITO substrate. Electrodeposition at mild negative potentials or for a short period of time yields a thin layer of sol-gel film, which acts
[20] as binder and facilitates the deposition of CNTs. Shifting the deposition potential more negative or prolonging the deposition time leads to more significant deposition of sol-gel component that further entraps the CNTs. The electrodeposition of sol-gel may occur to some extent on the surface of CNTs as they are
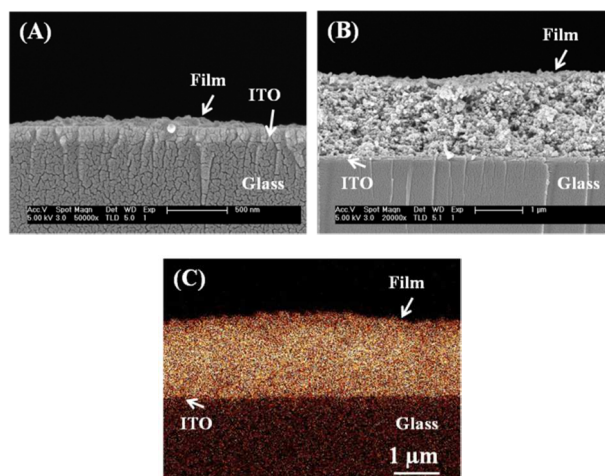[25] conductive.

Fig. 6 Cross-section SEM images of the sol-gel/CNT composite films electrodeposited at −0.75 V (A) and −1.2 V (B) for 2 min from Dispersion
[30] B. (C): EDX mapping of carbon for (B).

We recall that CNTs are also dip-coated from Dispersion A (Fig. 1B and 2A). To improve the selectivity of the electrodeposition process so that deposition is limited to the conductive surface, we reduced the viscosity of the deposition precursor. Dispersion B,
[35] which has lower concentration of NMP, was used for electrodeposition in the following work. The variations of film thickness and transmittance as a function of deposition potential and time (not shown) are similar to deposition from Dispersion A. The water contact angle of the electrodeposited films was
[40] measured (Fig. 5). The films are hydrophilic, as the contact angles measured are below 90°. Interestingly, the contact angle of the films decreases from 42° to 16° as the deposition potential is made negative, but it further increases to 27° at −1.3 V (Fig. 5A). Since the composition and surface energy of the films are
[45] unlikely to change significantly upon electrodeposition, the variation in contact angle is most probably related to the roughness of the films. From SEM images (Fig. 2), it can be seen that the roughness of the samples increases due to the film formation (especially the deposition of CNTs) at mild negative
[50] potentials. The increase in surface roughness of hydrophilic surfaces decreases the water contact angle as predicted by the Wenzel's relation. This could explain the decrease of the contact angle with negative potential shown in Fig. 5A. At more negative potentials, *e.g.* −1.3 V, we believe that the intensive deposition of
[55] silane fills the gaps between CNTs, thus reduces the roughness of the films leading to the slight increase in the contact angle. The contact angle of the films does not vary significantly with deposition time, although the film electrodeposited for 3 min shows slightly higher value (Fig. 5B). This suggests that the
[60] roughness of the films electrodeposited at −0.8 V is almost constant for the first 2.5 min and then begins to decrease due to the continuous deposition of silane.

The sol-gel/CNT composite films electrodeposited from Dispersion B were further characterized by cross-section
[65] SEM/EDX. The films were prepared on ITO and the cross-sections were obtained by breaking the samples. Fig. 6 shows the cross-section SEM images and EDX mapping of two typical silane films. It is seen from Fig. 6A that the film prepared at −0.75 V is very thin (< 100 nm). CNTs are not clearly seen in the
[70] film, indicating that they are lying parallel to the surface.
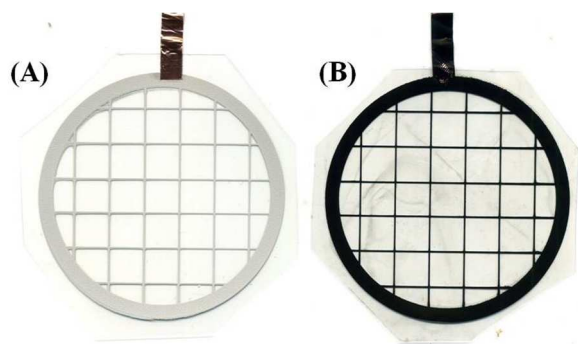
Fig. 7 Ag grid printed on PET before (A) and after (B) electrodeposition of sol-gel/CNT composite films at −0.9 V for 2 min from Dispersion B. The samples were scanned with white background.


5
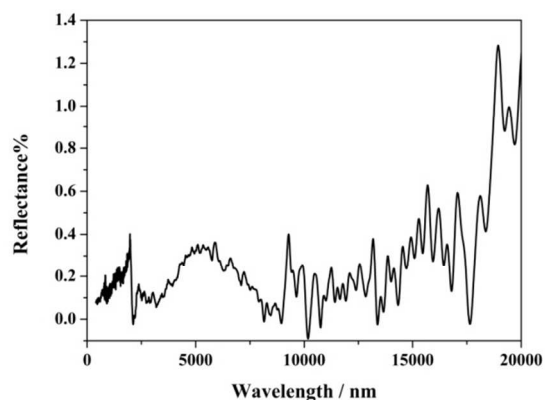
Fig. 8 Specular reflectance of sol-gel/CNT composite films electrodeposited on Ag printed on PET at -0.9 V for 2 min from Dispersion B.

Moreover, the film prepared at −1.2 V is much thicker, *ca.* 1.8
10 μm (Fig. 6B). Bright dots with diameter of *ca.* 50 nm are seen in the image, while tubular shaped CNTs are almost not observed. This suggests that also for this thickness CNTs are mostly in horizontal position embedded within the sol-gel matrix. EDX mapping of carbon reveals high carbon signals in the film, which
15 further confirms the presence of CNTs (Fig. 6C).

Besides the ease of manipulation by potential and time, another main advantage of the electrodeposition approach is the selective deposition on the conductive areas of a surface. Fig. 7 demonstrates this advantage by the electrodeposition of sol-
20 gel/CNT composite films on Ag grid printed on PET. The deposition was carried out in the optimized Dispersion B. It is evident that electrodeposition is predominantly limited to the conducting parts of the surface, namely to the Ag grid. The Ag grid turns black while the PET surface remains almost transparent.
25 The specular reflectance of the black film on Ag is below 0.5% in the spectrum range of 400 nm to 18 μm (Fig. 8). The low reflection is believed to be attributed to the high absorbance of CNTs. At the same time the transmittance of PET substrate remains 86%. These results indicate that the sol-gel/CNT
30 composite films, which can be used for antireflective coatings, can be selectively electrodeposited on conductive Ag surfaces.

We also examined the non-linear optical properties of the sol-gel/CNT composite films. Fig. 9 shows the transmittance of a typical electrodeposited sol-gel/CNT composite film as a function

35
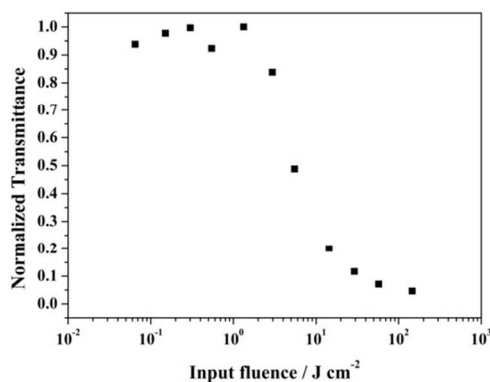
Fig. 9 Non-linear optical performance of sol-gel/CNT composite films electrodeposited on ITO at −0.9 V for 2 min from Dispersion B.

of the input fluence. The transmittance displayed is normalized to the maximum transmittance of the sample (T/T_{max}). As seen from
40 the figure, it decreases as the energy of the input laser increases, which is attributed to the non-linear effect of the films. It is known that the non-linear effect may arise from the absorption of nanostructured materials. Since electrodeposited silica film is white colored having low absorbance, the phenomenon is
45 attributed to the presence of CNTs in the film. The blank sample without silane had poor adhesion to the substrate, thus could not be measured, but similar non-linear effect was observed in CNT films with other binders. The fluence required for reducing the transmittance to 50% of its maximum value is 5.5 J/cm^2. These
50 results suggest that electrodeposited sol-gel/CNT composite films provide an alternative for non-linear optical materials, and they have much lower reflectance as compared with traditionally used metallic nanoparticles[54, 55].

Conclusions

55 The electrochemical co-deposition of nano-composites based on sol-gel and carbon nanotubes has been accomplished in a single electrochemical step. Applying a negative potential to the electrode caused the reduction of the protic solvent, altered the pH and catalyzed the deposition of sol-gel that entrapped the
60 CNTs inside the matrix. The deposition potential and time are the dominant factors that affect the thickness, transmittance and morphology of the films. Apparently, changing these parameters allows manipulating the deposition process and the properties of the films. Our results show that thicker films are electrodeposited
65 by applying more negative potential or depositing for longer time. The composite films are hydrophilic, and can be selectively electrodeposited on conductive surfaces. Finally, we demonstrated that the electrodeposited sol-gel/CNT composite films show good non-linear optical properties and pronounced
70 antireflection performance (blackness), which are mainly attributed to the high content of CNTs in the films. This work suggests electrodeposition as a powerful method of preparing sol-gel/CNT composite films for optical applications.

75

Notes and references

aInstitute of Chemistry, The Hebrew University of Jerusalem, Jerusalem 9190401, Israel. Fax: 972-2-6585319; Tel: 972-2-6585831; E-mail: daniel.mandler@mail.huji.ac.il
bSchool of Materials Science and Engineering, Nanyang Technological University, Singapore 639798, Singapore
cKiloLambda Technologies, Ltd., 22a Raoul Wallenberg St., Tel Aviv 61580, Israel.
dRafael Advanced Defense Systems, Ltd., POB 2250, Haifa 3102102, Israel

1. M. J. Biercuk, M. C. Llaguno, M. Radosavljevic, J. K. Hyun, A. T. Johnson and J. E. Fischer, *Appl. Phys. Lett.*, 2002, **80**, 2767-2769.
2. Z. Ounaies, C. Park, K. E. Wise, E. J. Siochi and J. S. Harrison, *Compos. Sci. Technol.*, 2003, **63**, 1637-1646.
3. M. C. Weisenberger, E. A. Grulke, D. Jacques, T. Rantell and R. Andrews, *J. Nanosci. Nanotech.*, 2003, **3**, 535-539.
4. P. Fournet, J. N. Coleman, B. Lahr, A. Drury, W. J. Blau, D. F. O'Brien and H. H. Horhold, *J. Appl. Phys.*, 2001, **90**, 969-975.
5. R. H. Baughman, C. X. Cui, A. A. Zakhidov, Z. Iqbal, J. N. Barisci, G. M. Spinks, G. G. Wallace, A. Mazzoldi, D. De Rossi, A. G. Rinzler, O. Jaschinski, S. Roth and M. Kertesz, *Science*, 1999, **284**, 1340-1344.
6. P. Gajendran and R. Saraswathi, *Pure Appl. Chem.*, 2008, **80**, 2377-2395.
7. W. Li, H. Jung, D. H. Nguyen, D. Kim, S. K. Hong and H. Kim, *Sens. Actuator B-Chem.*, 2010, **150**, 160-166.
8. W. D. Wang, P. Serp, P. Kalck and J. L. Faria, *Appl. Catal. B-Environ.*, 2005, **56**, 305-312.
9. S. Z. Kang, Z. Y. Cui and J. Min, *Fuller. Nanotub. Carbon Nanostruct.*, 2007, **15**, 81-88.
10. K. Woan, G. Pyrgiotakis and W. Sigmund, *Adv. Mater.*, 2009, **21**, 2233-2239.
11. M. Lu, M. K. Li, Z. J. Zhang and H. L. Li, *Appl. Surf. Sci.*, 2003, **218**, 195-201.
12. A. Star, J. F. Stoddart, D. Steuerman, M. Diehl, A. Boukai, E. W. Wong, X. Yang, S. W. Chung, H. Choi and J. R. Heath, *Angew. Chem. Int. Ed.*, 2001, **40**, 1721-1725.
13. M. Moniruzzaman and K. I. Winey, *Macromolecules*, 2006, **39**, 5194-5205.
14. M. Baibarac and P. Gomez-Romero, *J. Nanosci. Nanotech.*, 2006, **6**, 289-302.
15. J. Li, S. B. Tang, L. Lu and H. C. Zeng, *J. Am. Chem. Soc.*, 2007, **129**, 9401-9409.
16. V. G. Gavalas, R. Andrews, D. Bhattacharyya and L. G. Bachas, *Nano Lett.*, 2001, **1**, 719-721.
17. Q. Zhao, M. B. Nardelli, W. Lu and J. Bernholc, *Nano Lett.*, 2005, **5**, 847-851.
18. E. Kymakis, I. Alexandrou and G. A. J. Amaratunga, *J. Appl. Phys.*, 2003, **93**, 1764-1768.
19. S. H. Qin, D. Q. Qin, W. T. Ford, D. E. Resasco and J. E. Herrera, *Macromolecules*, 2004, **37**, 752-757.
20. Y. H. Hu and S. B. Sinnott, *J. Mater. Chem.*, 2004, **14**, 719-729.
21. C. Velasco-Santos, A. L. Martinez-Hernandez and V. M. Castano, *Compos. Interfaces*, 2005, **11**, 567-586.
22. F. Yakuphanoglu, I. S. Yahia, G. Barim and B. F. Senkal, *Synth. Met.*, 2010, **160**, 1718-1726.
23. J. X. Zeng, X. H. Gao, W. Z. Wei, X. R. Zhai, J. Yin, L. Wu, X. Y. Liu, K. Liu and S. G. Gong, *Sens. Actuator B-Chem.*, 2007, **120**, 595-602.
24. V. Branzoi, L. Pilan and F. Branzoi, *Electroanalysis*, 2009, **21**, 557-562.
25. P. Hojati-Talemi and G. P. Simon, *J. Phys. Chem. C*, 2010, **114**, 13962-13966.
26. R. X. Zhang, L. Z. Fan, Y. P. Fang and S. H. Yang, *J. Mater. Chem.*, 2008, **18**, 4964-4970.
27. J. Sun and L. Gao, *J. Electroceram.*, 2006, **17**, 91-94.
28. H. Ren, Y. Y. Liu, Q. J. Jiao, X. F. Fu and T. T. Yang, *J. Phys. Chem. Solids*, 2010, **71**, 149-152.
29. H. Q. Li, C. S. Ha and I. Kim, *Nanoscale Res. Lett.*, 2009, **4**, 1384-1388.
30. D. Eder, *Chem. Rev.*, 2010, **110**, 1348-1385.
31. L. L. Hench and J. K. West, *Chem. Rev.*, 1990, **90**, 33-72.
32. N. Husing and U. Schubert, *Angew. Chem. Int. Ed.*, 1998, **37**, 23-45.
33. Y. J. Zhang, Y. F. Shen, D. X. Han, Z. J. Wang, J. X. Song and L. Niu, *J. Mater. Chem.*, 2006, **16**, 4592-4597.
34. J. W. Wang, M. Gu, J. W. Di, Y. S. Gao, Y. Wu and Y. F. Tu, *Bioprocess. Biosyst. Eng.*, 2007, **30**, 289-296.
35. M. Vila, J. L. Hueso, M. Manzano, I. Izquierdo-Barba, A. de Andres, J. Sanchez-Marcos, C. Prieto and M. Vallet-Regi, *J. Mater. Chem.*, 2009, **19**, 7745-7752.
36. L. Berguiga, J. Bellessa, F. Vocanson, E. Bernstein and J. C. Plenet, *Opt. Mater.*, 2006, **28**, 167-171.
37. R. Shacham, D. Avnir and D. Mandler, *Adv. Mater.*, 1999, **11**, 384-388.
38. J. M. Hu, L. Liu, J. Q. Zhang and C. N. Cao, *Electrochim. Acta*, 2006, **51**, 3944-3949.
39. J. M. Hu, L. Liu, J. Q. Zhang and C. N. Cao, *Prog. Org. Coat.*, 2007, **58**, 265-271.
40. P. N. Deepa, M. Kanungo, G. Claycomb, P. M. A. Sherwood and M. M. Collinson, *Anal. Chem.*, 2003, **75**, 5399-5405.
41. M. M. Collinson, D. A. Higgins, R. Kommidi and D. Campbell-Rance, *Anal. Chem.*, 2008, **80**, 651-656.
42. A. Walcarius, E. Sibottier, M. Etienne and J. Ghanbaja, *Nat. Mater.*, 2007, **6**, 602-608.
43. R. Toledano, R. Shacham, D. Avnir and D. Mandler, *Chem. Mater.*, 2008, **20**, 4276-4283.
44. L.-K. Wu, J.-M. Hu and J.-Q. Zhang, *Corros. Sci.*, 2012, **59**, 348-351.
45. R. Toledano and D. Mandler, *Chem. Mater.*, 2010, **22**, 3943-3951.
46. M. Kanungo, H. S. Isaacs and S. S. Wong, *J. Phys. Chem. C*, 2007, **111**, 17730-17742.
47. V. Urbanova, M. Etienne and A. Walcarius, *Electroanalysis*, 2013, **25**, 85-93.
48. M. A. Aziz and H. Yang, *Chem. Commun.*, 2008, 826-828.
49. C. Sanchís, Á. Berenguer-Murcia, R. Ruiz-Rosas, E. Morallón and D. Cazorla-Amorós, *Carbon*, 2014, **67**, 564-571.
50. R. Cai, H. Freiser and S. Muralidharan, *Langmuir*, 1995, **11**, 2926-2930.
51. R. Okner, G. Favaro, A. Radko, A. J. Domb and D. Mandler, *Phys. Chem. Chem. Phys.*, 2010, **12**, 15265-15273.
52. E. Gdor and D. Mandler, *J. Mater. Chem.*, 2011, **21**, 12145-12150.
53. M. Raveh, L. Liu and D. Mandler, *Phys. Chem. Chem. Phys.*, 2013, **15**, 10876-10884.
54. A. L. Stepanov, C. Marques, E. Alves, R. C. da Silva, M. R. Silva, R. A. Ganeev, A. I. Ryasnyansky and T. Usmanov, *Tech. Phys. Lett.*, 2005, **31**, 702-705.
55. A. L. Stepanov, *Rev. Adv. Mater. Sci.*, 2011, **27**, 115-145.

Table of Contents Entry

This work reports a method of electrodepositing sol-gel/CNT composite films. The deposition is highly selective to conductive surfaces, and the films show non-linear optical properties and excellent antireflection performance.

Keywords: electrodeposition, carbon nanotubes, silane, non-linear optics, antireflection coatings